

Article

Antioxidant Activity and Volatile Oil Analysis of Ethanol Extract of *Phoebe zhennan* S. Lee et F. N. Wei Leaves

Liping Yu ^{1,†}, Wang Cheng ^{1,†}, Meifen Tian ², Zhigang Wu ^{1,3,*}, Xiaoli Wei ^{1,*}, Xing Cheng ⁴, Mingwei Yang ⁵ and Xuan Ma ⁵

¹ College of Forestry, Guizhou University, Guiyang 550025, China; ylpgz@163.com (L.Y.); 13638526017@163.com (W.C.)

² Xifeng County Bureau of Natural Resources, Guiyang 551100, China; 18302687749@163.com

³ International Joint Research Center for Biomass Materials, Southwest Forestry University, Kunming 650224, China

⁴ Dozheng County Bureau of Forestry, Zunyi 563500, China; 18385130273@163.com

⁵ Zhejiang Academy of Forestry, Hangzhou 310000, China; wing_yang1978@sina.com (M.Y.); jwmax66@163.com (X.M.)

* Correspondence: zgwu1@gzu.edu.cn (Z.W.); gdwxl-69@126.com (X.W.); Tel.: +86-851-8829-8397 (X.W.)

† These authors contributed equally to this work.

Abstract: The medicinal value of *P. zhennan* has been documented in traditional Chinese medicine books. The aim of this paper was to study the antioxidant activity of alcoholic extracts of *P. zhennan* leaves using 1,1-diphenyl-2-picrylhydrazyl (DPPH) and 2-phenyl-4,4,5,5-tetramethylimidazoleoxyl-1-oxyl-3-oxide (PTIO) radical scavenging and ferric ion reducing antioxidant power (FRAP) assays. The active components of the leaves were identified via headspace solid-phase microextraction and gas chromatography–mass spectrometry (HS-SPME-GC-MS). The results showed that the scavenging rate of DPPH was 94.67% with an EC₅₀ value of 0.674 mg/mL at a concentration of 2 mg/mL. The maximum scavenging rate was 47.40% at a Trolox equivalent of 0.33 mg TE/mL for PTIO radicals. The FRAP reached 84.80% at 0.20 mg/mL concentration. The results confirmed the strong antioxidant activity of the extracts. Furthermore, 44 compounds, mostly terpenoids, obtained from the alcoholic extracts of *P. zhennan* leaves were analyzed using HS-SPME-GC-MS and 15 of these compounds had a relative content exceeding 1%. The strong antioxidant activity of the alcoholic extracts of *P. zhennan* leaves could be attributed to the presence of copaene (33.97%), β-caryophyllene (4.42%), δ-cadinene (11.04%), γ-murolene (4.78%), cis-calamenene (2.02%), linalool (1.04%), α-pinene (1.46%), borneol acetate (1.5%), and γ-terpinene (0.66%). This study demonstrates the potential medicinal value of alcoholic extracts of *P. zhennan* leaves.

Keywords: *P. zhennan*; antioxidant activity; free radical scavenging activity; HS-SPME-GC-MS



Citation: Yu, L.; Cheng, W.; Tian, M.; Wu, Z.; Wei, X.; Cheng, X.; Yang, M.; Ma, X. Antioxidant Activity and Volatile Oil Analysis of Ethanol Extract of *Phoebe zhennan* S. Lee et F. N. Wei Leaves. *Forests* **2024**, *15*, 236. <https://doi.org/10.3390/f15020236>

Academic Editor: Frank S. Gilliam

Received: 30 November 2023

Revised: 2 January 2024

Accepted: 23 January 2024

Published: 26 January 2024



Copyright: © 2024 by the authors. Licensee MDPI, Basel, Switzerland. This article is an open access article distributed under the terms and conditions of the Creative Commons Attribution (CC BY) license (<https://creativecommons.org/licenses/by/4.0/>).

1. Introduction

Phoebe zhennan is a member of the Lauraceae family; its use in infectious, internal, and dermatological diseases is clearly documented in traditional Chinese pharmacological books, such as *Zheng lei ben cao*, *Taiping Shenghui Fang*, and *Puji Fang*. Numerous studies have shown that antioxidant can effectively prevent aging and many diseases. Antioxidation is the abbreviation of antioxidant free radicals. When the human body is in continuous contact with the external environment, free radicals are continuously produced in the body through factors such as respiration (oxidation reaction), external pollution, and radiation exposure. Free radicals break down cells and tissues, affecting metabolic function and causing varying degrees of health problems. For example, common cancers [1], aging [2], diabetes [3], respiratory diseases [4], nervous system diseases [5], and so on are all related to oxidative free radicals. If excessive oxidative free radicals are eliminated, many aging and related diseases caused by free radicals can be prevented. Many natural plant extracts

have been shown to have antioxidant activity, so the search for plant-derived antioxidants is increasing [6–8]. However, there are few reports on the antioxidant activity of *P. zhennan*. The antioxidant activity can be reflected by an in vitro antioxidant activity test, that is, the scavenging ability of the tested samples to synthetic free radicals is evaluated [9–12]. Common artificial free radicals include 1,1-diphenyl-2-picrylhydrazyl radical (DPPH), ABTS radical, 3-oxo-2-phenyl-4,4,5,5-tetramethylimidazoline-1-oxygen radical (PTIO) [13–15], etc. The determination of iron ion reducing power (FARP) is also a common method to evaluate antioxidant activity [16]. The evaluation indexes of free radical scavenging activity include free radical scavenging rate, half inhibitory concentration (IC50) [17], half effective concentration (EC50), and Trolox equivalent [18–22].

The antioxidant activity of a plant is related to the chemical composition of the extract. Traditional extraction methods all suffer from low extraction efficiency and a serious waste of resources. However, as an emerging plant extraction method, ultrasonic-assisted extraction technology accelerates extraction efficiency, saves energy, and protects the environment. It is regarded as a “green technology” and has been widely used to extract and separate active ingredients in plants. In this study, absolute ethanol was used to extract the active ingredients of *P. zhennan* leaves via ultrasonic technology. Headspace solid-phase microextraction and gas chromatography–mass spectrometry (HS-SPME-GC-MS) technology was used to analyze the active ingredients in *P. zhennan* leaves to clarify their mechanism of action further. Based on the record of its medical effects in traditional Chinese pharmaceutical works, this study explores the novelty and significance of its antioxidant activity.

2. Materials and Methods

2.1. Materials

The leaves of *Phoebe zhennan* S. Lee et F. N. Wei were harvested on 18 October 2021, from QingLang Village, Zhouxi Town, Kaili City, Guizhou Province, China (107.8679997 E, 26.4462369 N). The main reagents used were DPPH, water-soluble vitamin E (Trolox), PTIO, dihydrogen phosphate, sodium chloride, 1% potassium ferricyanide, 10% trichloroacetic acid solution, 0.1% ferric chloride solution, and anhydrous ethanol. All reagents were analytically pure and bought from Shanghai Aladdin Biochemical Technology Co. (Shanghai, China).

The main instruments and equipment used were an SY-2000 rotary evaporator (Shanghai Yarong Biochemical Instrument Factory; Shanghai, China), a 7890A-5975C gas chromatograph (Agilent Technologies; Santa Clara, CA, USA), and 50/30 μm PDMS/CAR/DVB (2 cm) extraction fiber (Supelco; Bellefonte, PA, USA).

2.2. Ultrasonic-Assisted Ethanol Extraction

After picking the samples, the leaves of *P. zhennan* were placed in a clean, cool, and dry place to dry in the shade. Dried leaves of the appropriate quantity were crushed and passed through a 60-mesh sieve. Thereafter, a 15 g sample was transferred into a 250 mL wide-mouth bottle, and anhydrous ethanol was added as the extraction solution. The extraction was repeated three times; the extract was centrifuged at 3000 r/min for 10 min and then vacuum filtered and concentrated with a rotary evaporator.

2.3. DPPH Radical Scavenging Assay

We used the reference [13] method with slight modifications. Exactly 6.9 mg of the DPPH standard sample was weighed and dissolved in anhydrous ethanol to make a final volume of 250 mL under light-proof conditions. Anhydrous ethanol was used as the blank control. The absorbance (OD) was measured at 517 nm for 30 min after the reaction under light-proof conditions, with three replicates. The concentration of the DPPH solution on the X-axis and the OD value on the Y-axis gave the DPPH standard curves.

Different concentrations of the alcoholic extracts of *P. zhennan* and Trolox standard (water-soluble vitamin E) solutions were also prepared. Measure the absorbance of the DPPH solution as A_1 . Measure the absorbance of the experimental group (*P. zhennan* and

Trolox) as A . Measure the blank absorbance of the sample as A_0 . The above measurements were zeroed with anhydrous ethanol, and the free radical scavenging rate was calculated using the formula shown in the following equation. The EC50 was calculated using GraphPad Prism 9 software (Graphstats Technologies, Bengaluru, India).

$$\text{Scavenging Rate of DPPH Radical (\%)} = \frac{A_1 - (A - A_0)}{A_1} \times 100\%$$

2.4. PTIO Radical Scavenging Assay

We used the method described in the literature [15] with slight modifications. The PTIO solution was prepared by weighing 45 mg of the PTIO standard sample and fixing the volume to 200 mL with anhydrous ethanol; it was stored at 4 °C until use. Trolox standard solutions were prepared at concentrations of 4, 2, 1, 0.5, 0.25, and 0.125 mg/mL, and the scavenging rate of PTIO radicals by Trolox at different concentrations was determined. The Trolox standard curves were plotted with the Trolox concentration as the X-axis and the scavenging rate as the Y-axis. The different concentrations of the alcohol extract solution of *P. zhennan* leaves were configured sequentially. The absorbance was measured at 557 nm after a 30 min reaction at 37 °C in a water bath. Measure the absorbance of the PTIO solution as A_1 . Measure the absorbance of the experimental group (*P. zhennan* and Trolox) as A . Measure the blank absorbance of the sample as A_0 . The above measurements were zeroed with anhydrous ethanol, and each measurement was repeated 3 times to calculate the free radical scavenging rate using the formula shown in the following equation.

$$\text{Scavenging Rate of PTIO Radical (\%)} = \frac{A_1 - (A - A_0)}{A_1} \times 100\%$$

2.5. PRAP Assay

The reference method [16] was used with slight modifications. We made a 0.2 mol/L phosphate-buffered solution (pH = 6.6). Then, 1.74 g of sodium dihydrogen phosphate, 2.7 g of disodium hydrogen phosphate, and 1.7 g of sodium chloride with an analytical balance were dissolved in distilled water, and the volume was made up to 400 mL. A 1 mL aliquot each of 0.2 mol/L phosphate buffer and 1% potassium ferricyanide solution was added to 1.2 mL each of 0.05, 0.1, 0.15, 0.2, 0.25, and 3 mg/mL concentrations of selenium alcohol extract. The resulting mixture was placed in a constant-temperature water bath at 50 °C for 20 min and then cooled rapidly. Then, we added 1 mL of a 10% trichloroacetic acid solution and centrifuged at 3000 r/min for 10 min.

Further, we added 0.5 mL of 0.1% ferric chloride solution to 2.5 mL of the supernatant, mixed well, and added distilled water to obtain a final volume of 5 mL. Absorbance A was measured at 700 nm after 10 min. The solvent was replaced with distilled water to determine the absorbance of the sample blank A_0 ; the absorbance of the test control was recorded as A_1 , and Trolox was used as the positive control. Three replicates of each measurement were used to calculate the ferric ion-reducing capacity using the formula in the following equation.

$$\text{FRAP (\%)} = \frac{A - A_1 - A_0}{A} \times 100\%$$

2.6. HS-SPME-GC-MS Analysis

Sample treatment: To perform HS-SPME-GC-MS, the leaves were crushed separately and sieved through a 60-mesh sieve; 1 g of leaf powder was weighed into a 15 mL extraction vial and sealed quickly. The fiber head was aged at 250 °C in the GC-MS inlet until there were no spurious peaks. The sample vial was placed in the SPME device, and the temperature was set at 35 °C. The sample vial was placed in the extraction device to preheat for 15 min, and the SPME head was inserted into the headspace portion of the sample through the vial cap. The fiber head was pushed out. The extraction head was

approximately 1.0 cm above the upper surface of the sample, and the headspace extraction was performed for 40 min. The fiber head was withdrawn, and the extraction head was pulled out of the sample vial. Then, the extraction head was inserted into the GC-MS inlet, the fiber head was pushed out, and the sample was analyzed at 250 °C for 3 min.

Chromatographic conditions: The chromatographic column used was DB-WAX (30.0 m × 250 μm, 0.25 μm). The column was started at 40 °C and held for 5 min, ramped up to 180 °C at 10 °C/min, held for 5 min, and then ramped up at 20 °C/min to 250 °C. The gas chamber temperature was 250 °C, and the transfer line temperature was 250 °C. The carrier gas was He, and the carrier gas flow rate was 1.0 mL/min; there was no shunt.

Mass spectrometer conditions: EI source; electron energy 70 eV; ion source temperature 230 °C; quadrupole 150 °C; scan mode Scan; scan mass range 35–550 μ.

Qualitative and quantitative analyses: Using the MS database NIST11, we detected the retention time and retention index. Database screening of the results was performed to deduct parameters such as column loss peak. The area normalization method was used to quantify the quantitative results, i.e., the percentage of the peak area of the identified component to the sum of the areas of all identified components. The following formula was used:

$$C_i = \frac{A_i}{A_1 + A_2 \cdots + A_i + A_n} \times 100\%$$

where:

C_i = content of an identified component, %;

A_i = the peak area corresponding to an identified component;

n = the total number of identified components.

3. Results and Discussion

3.1. DPPH Radical-Scavenging Activities

The DPPH standard curve is shown in Figure 1A, and the fitted equation is $Y = 0.008058X + 0.003886$, $R^2 = 0.9966$. The absorbance of DPPH was significantly linearly correlated with the concentration. According to Beer's law, the spectrophotometer transmission ratio has the highest accuracy in the range of 20% to 60% absorbance [23], i.e., absorbance in the range of 0.222–0.699 is appropriate. The analytical equation showed that the absorbance was 0.555 Abs when the concentration was 70 μmol/L, which met the accuracy requirement. Thus, the concentration was selected for the subsequent test.

The scavenging ability of DPPH radicals and the correlation between the two at different concentrations of the alcoholic extracts of *P. zhennan* leaves are shown in Figures 1 and 2. As shown in Figures 1B and 2C, with Trolox as the positive control, trolox at 0.125–4 mg/mL had a scavenging rate of approximately 96.41%, and it showed strong antioxidant activity. The concentration-dependent scavenging rate of DPPH by the alcoholic extracts of *P. zhennan* leaves was extremely significant ($p < 0.0001$) before reaching 2 mg/mL, and the scavenging rate reached 49.04% when the concentration was 0.125 mg/mL. The scavenging rate increased rapidly with increasing concentration. As the concentration increased to 2 mg/mL, the scavenging rate of DPPH by the alcoholic extracts of *P. zhennan* leaves reached 94.67% and then became stable. This was only 1.74% lower than Trolox's scavenging rate of 96.41%, indicating that the scavenging effect of Siberian hemlock alcoholic extracts on DPPH was significant. Considering the utilization rate and scavenging effect, the optimal concentration of DPPH radicals scavenged by the alcoholic extracts of *P. zhennan* leaves was 2 mg/mL.

EC50 is the antioxidant concentration that reduces the concentration of DPPH free radicals by 50%; the lower the EC50 value, the stronger the scavenging ability. The EC50 value for DPPH free radicals from the alcoholic extract of *P. zhennan* leaves was 0.674 mg/mL, as calculated using the regression model in the program GraphPad Prism 9 (Figure 1D). According to the results, Wild Z. spina-christi of Ethiopia and Z. jujube fruit species of India are rich in antioxidant elements, such as magnesium, zinc, and selenium. They have been reported to have an EC50 of 2.94–7.75 mg/mL of DPPH free radicals [24,25].

In contrast, the EC₅₀ of the alcoholic extract of *P. zhennan* leaves is only 8.69%–22.92% of theirs, which somehow corresponds to a decrease of 77.08%–91.31%. The analysis of its bioactive components also suggests that it could be a potential antioxidant.

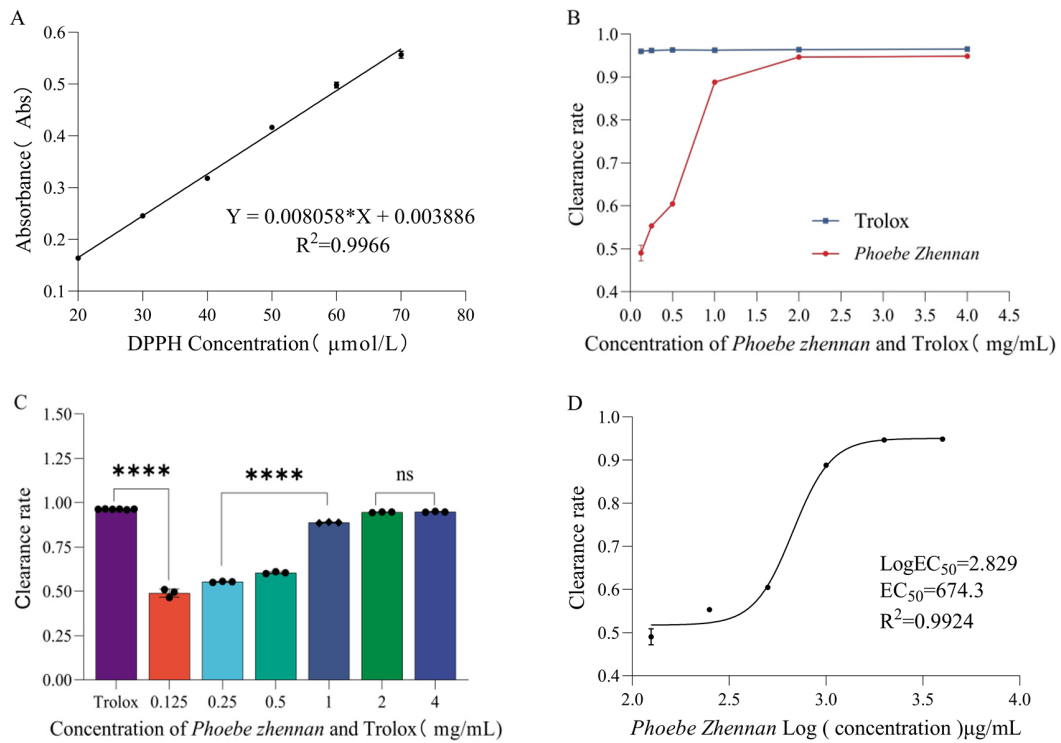


Figure 1. (A) The DPPH standard curve. (B) The dose–effect curve of Trolox and *P. zhennan* to DPPH. (C) Correlation analysis of the DPPH scavenging rate between Trolox and *P. zhennan* at different concentrations. ****, significant difference ($p < 0.0001$); ns, no significant difference ($p > 0.05$). (D) The EC₅₀ of *P. zhennan* on DPPH.

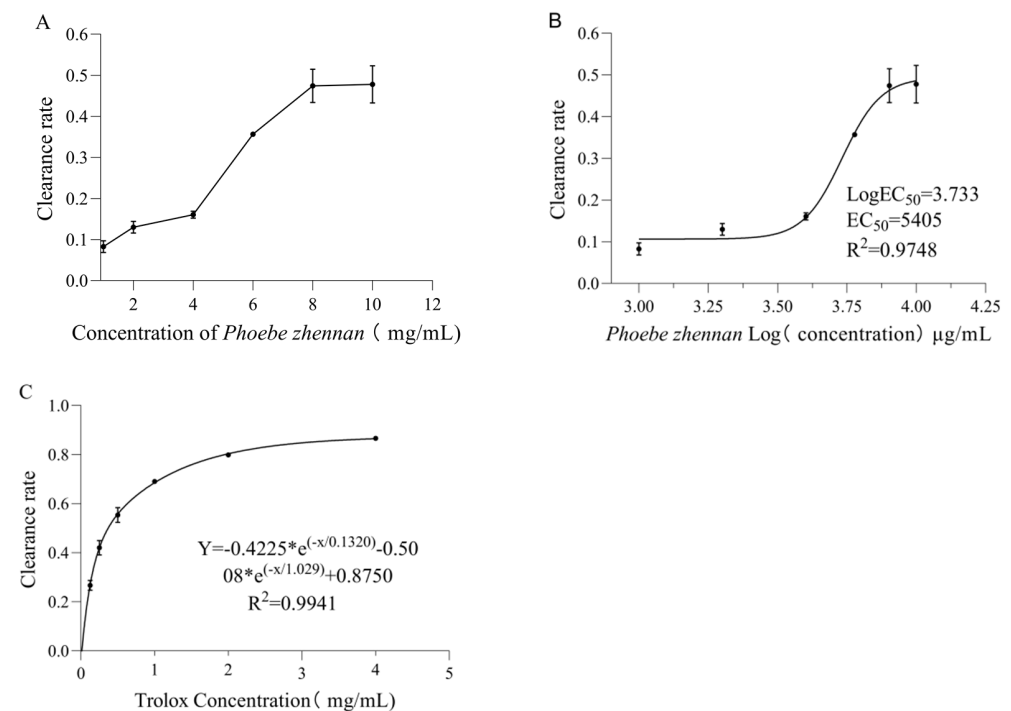


Figure 2. (A) The dose–effect curve of *P. zhennan* to PTIO. (B) The EC₅₀ of *P. zhennan* on DPPH. (C) The clearance rate of PTIO by Trolox.

3.2. PTIO Radical-Scavenging Activities

The color of the PTIO solution is bluish purple, which fades when it reacts with antioxidants. PTIO solution has a strong absorption peak at 557 nm. The absorbance of PTIO at a concentration of 0.225 mg/mL was tested to be 0.347, which conforms to Beer's law; thus, this concentration was chosen for the test. The results of PTIO radical-scavenging activities were shown in Figure 2. As shown in Figure 2A, the scavenging effect of PTIO radical scavenging increases slowly with increasing concentration when the concentration is below 4 mg/mL, with a linear fit slope of 0.02445 and $R^2 = 0.8203$. In the range of 4–8 mg/mL, the linear fit slope is 0.07837 and $R^2 = 0.9572$, with strong linearity of the quantitative-efficacy relationship. The scavenging rate increased rapidly, approximately 3.2 times that at concentrations below 4 mg/mL. At 8 mg/mL concentration, the scavenging rate reached 47.40 %, followed by a flattening of the quantitative-efficacy curve, indicating a maximum scavenging rate of 47.79 % for free radicals. The scavenging rate of PTIO by the extract of *P. zhennan* leaves at maximum concentration is similar to that of the water extracts of six traditional Chinese medicine plants selected in the experiment by Li [15], including *Angelicae sinensis* radix, at similar concentrations.

As shown in Figure 2B, the EC_{50} value of the ethanol extract of *P. zhennan* leaves to PTIO free radical was 5.405 mg/mL by regression model calculation. As shown in Figure 2C, PTIO is more stable than DPPH, and Trolox reaches an 86.63% scavenging rate only at a concentration of 4 mg/mL. The fitted equation for the scavenging rate of PTIO radicals by Trolox is $Y = -0.4225e^{-x/0.1320} - 0.5008e^{-x/1.029} + 0.8750$, $R^2 = 0.9941$. The antioxidant capacity can be reflected by the TEAC, which compares the antioxidant capacity of a given substance with that of the standard antioxidant substance Trolox. The higher the TEAC value, the higher the antioxidant capacity. The TEAC for PTIO radical scavenging ability of the alcoholic extracts of *P. zhennan* leaves was found to be 0.33 mg TE/mL.

3.3. PRAP Test Analysis

The ferric ion reduction method refers to the ability of the sample to reduce the trivalent iron of potassium ferricyanide to divalent iron, yielding potassium ferrocyanide. Under acidic conditions, potassium ferricyanide reacts with ferric chloride to form ferricyanide, which has an absorption peak at 700 nm. The stronger the reducing ability of the sample is, the higher the absorbance at 700 nm, and the stronger the antioxidant performance is. The reducing ability of ferric ions is shown in Figure 3A. The figure shows that the reducing ability of Trolox increases with concentration and reaches a strong reducing ability of 94.98% at a concentration of 0.25 mg/mL. In contrast, the ferrous ion reduction capacity of the alcoholic extract of the leaves of *P. zhennan* increased with increasing concentration and then slightly decreased and stabilized at concentrations above 0.20 mg/mL. The highest reducing capacity of the alcoholic extract of *P. zhennan* leaves was 84.80%, which was lower than that of the positive control Trolox; however, the extract had a strong reducing capacity, proving its strong antioxidant capacity. As shown in Figure 3B, the fitting equation of Trolox PRAP is $Y = -246.1 + (0.9462 + 246.1)/(1 + 10^{-(0.3684 - x) \times 8.026})$, $R^2 = 0.9816$. Through analysis, the Trolox equivalent was 0.03 mg TE/mL when the iron ion reduction ability of *P. zhennan* ethanol extract reached its maximum. It is worth noting that the research results proposed by Wojtunik [26] indicate that in the case of spectrophotometric determination, isoterpenol and linalool exhibit high reducing activity. In addition, α -terpenes, γ -terpenes, and other compounds have reducing activity. This is consistent with the composition analysis in the following text, which mainly focuses on terpenoids. Therefore, the abundance of terpenoids can be considered as the reason for the reducing ability of *P. zhennan* leaves. However, further investigation is needed.

3.4. Active Constituents

The HS-SPME-GC-MS total ion flow diagram is shown in Figure 4. There are many peaks in the volatile component spectrum of *P. zhennan* leaves. These peaks were searched with the NIST database. As described in Section 2.6, impurity peaks such as polyoxysilane

(the column loss component) are subtracted and normalized using the area method. A total of 99 compounds were obtained from the leaves using HS-SPME-GC-MS, and 44 compounds were analyzed for each compound after excluding the data with a match lower than 80%. Among them, there are 21 kinds of sesquiterpenes, 6 kinds of alkenes, 7 kinds of monoterpenes, 2 kinds of monoterpene alcohols, 3 kinds of aromatic hydrocarbons, 1 kind of acid, 1 kind of aromatic ester, and 3 other kinds.

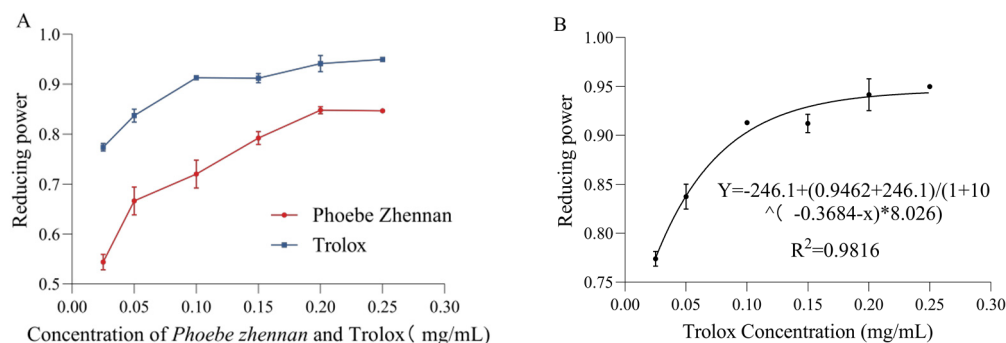


Figure 3. (A) The reduction ability of *P. zhennan* and Trolox; (B) The EC₅₀ of *P. zhennan* on PRAP.

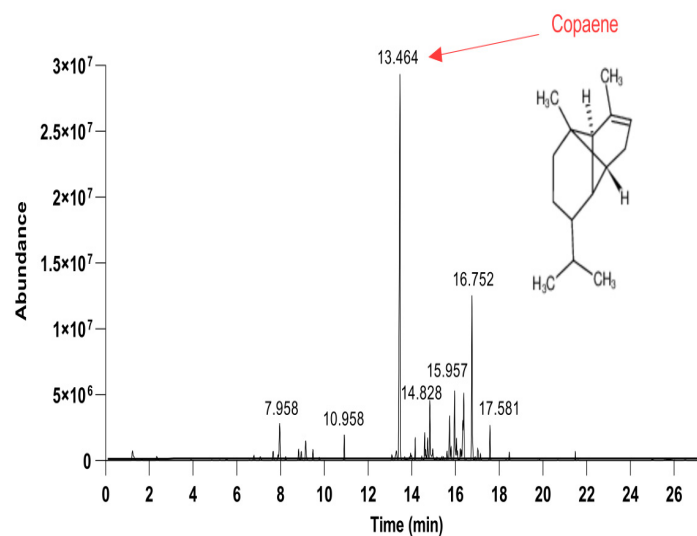


Figure 4. TIC of volatile components in *P. zhennan* leaves.

A total of 15 compounds had a relative content of more than 1%, and the highest relative content was copaene (33.97%). Other compounds included δ -cadinene (11.04%), γ -muurolene (4.78%), α -muurolene (4.68%), β -caryophyllene (4.42%), and eucalyptol (3.31%), 1,4,7,-cycloundecatriene, 1,5,9,9-tetramethyl-, Z,Z,Z- (2.99%), cis-calamenene (2.02%), β -elemene (1.7%), benzocyclobutene (1.63%), borneol acetate (1.5%), α -pinene (1.46%), ylangene (1.34%), β -patchoulene (1.07%), and linalool (1.04%), as detailed in Table 1. The active ingredients in *P. zhennan* leaves are mostly terpenoids. These terpenoids possess similar structures and activities, such as bacteriostatic, anticancer, and antioxidant qualities.

Copaene, γ -muurolene, and δ -cadinene were also reported in the bark of *Cinnamomum loureirii* from the Lauraceae family. Copaene, γ -muurolene, and δ -cadinene are sesquiterpenes, and their contents are significantly and positively correlated with the antioxidant activity of FRAP and ABTS [27]. Studies have shown that many sesquiterpenes have good antioxidant activity and antibacterial effects. As the most abundant sesquiterpene in this study, copaene is widely found in many plants [28,29] and has antibacterial and antioxidant properties [30]. Its chemical properties are active, and it has a variety of reaction capabilities and great potential for modification. It can prepare a variety of derivatives, and its derivatives also have anti-tumor cell proliferation activity [31,32]. It can also synthesize flame

retardants, sweeteners, plasticizers, attractants, functional materials, etc. [33]. Therefore, the product development of copaene and its derivatives has become the focus. *cis*-Calamenene is a sesquiterpene; along with α -pinene, it is also a major component of plants such as *Juniperus oxycedrus* that have good antioxidant activity [34,35]. β -Caryophyllene is a natural terpene. Caryophyllene is a natural bicyclic sesquiterpene with strong antioxidant activity. Dahham reported that caryophyllene's IC₅₀ values for DPPH and FRAP were 1.25 and 3.23 μ M, respectively [36]. Linalool is an oxygenated monoterpene with an EC₅₀ of only 6.78 μ g/mL for ABTS [37]; this reveals the pharmacological potential of linalool.

Table 1. Main active components and relative contents of *P. zhennan* leaves.

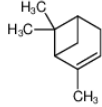
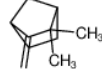
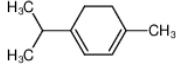
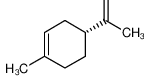
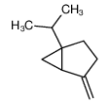
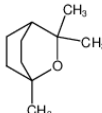
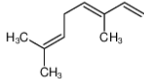
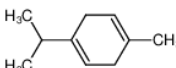
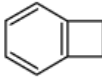
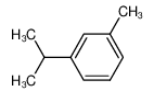
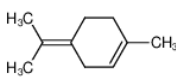
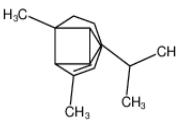
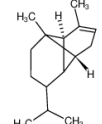
NO.	TR/min	Compound	MW	CAS	Content/%	Structure
1	1.24	α -Pinene	136.12	80-56-8	1.46	
2	2.35	Camphene	136.12	79-92-5	0.48	
3	7.08	α -Terpinene	136.12	99-86-5	0.47	
4	7.66	D-Limonene	136.12	5989-27-5	0.88	
5	7.89	(\pm)-Sabinene	136.12	3387-41-5	0.48	
6	7.96	Eucalyptol	154.14	470-82-6	3.31	
7	8.83	<i>trans</i> - β -Ocimene	136.12	3779-61-1	0.82	
8	8.95	γ -Terpinene	136.12	99-85-4	0.66	
9	9.15	Benzocyclobutene	104.06	694-87-1	1.63	
10	9.48	<i>m</i> -Cymene	134.11	535-77-3	0.74	
11	9.78	Terpinolene	136.12	586-62-9	0.23	
12	13.3	Ylangene	204.19	14912-44-8	1.34	
13	13.46	Copaene	204.19	3856-25-5	33.97	

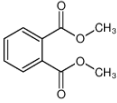
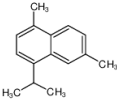
Table 1. Cont.

NO.	TR/min	Compound	MW	CAS	Content/%	Structure
14	13.79	β -Bourene	204.19	5208-59-3	0.09	
15	13.9	Alloaromadendrene	204.19	17334-55-3	0.26	
16	13.95	(-)- α -Gurjunene	204.19	489-40-7	0.51	
17	13.99	(+)-Sativene	204.19	3650-28-0	0.38	
18	14.16	Linalool	154.14	78-70-6	1.04	
19	14.46	α -Bergamotene	204.19	17699-05-7	0.41	
20	14.59	Borneol acetate	196.15	5655-61-8	1.5	
21	14.64	Fenchol	154.14	1632-73-1	0.52	
22	14.68	Zingiberene	204.19	495-60-3	0.27	
23	14.73	β -Elemene	204.19	110823-68-2	1.7	
24	14.83	β -Caryophyllene	204.19	87-44-5	4.42	
25	14.96	β -Patchoulene	204.19	514-51-2	1.07	
26	15.16	α -Elemene	204.19	5951-67-7	0.3	
27	15.38	(+)- γ -Cadinene	204.19	39029-41-9	0.39	

Table 1. Cont.

NO.	TR/min	Compound	MW	CAS	Content/%	Structure
28	15.45	Aromandendrene	204.19	489-39-4	0.27	
29	15.73	1,4,7,- Cycloundecatriene, 1,5,9,9-tetramethyl-, Z,Z,Z-	204.19	1000062-61- 9	2.99	
30	15.8	2-Isopropenyl-4a,8- dimethyl- 1,2,3,4,4a,5,6,7- octahydronaphthalene	204.19	1000192-43- 5	0.92	
31	15.96	γ -Muurolene	204.19	30021-74-0	4.78	
32	16.09	(+)-Borneol	154.14	1000150-76- 3	0.47	
33	16.22	Isoledene	204.19	1000156-10- 8	0.76	
34	16.38	α -Muurolene	204.19	31983-22-9	4.68	
35	16.53	Cedr-8-ene	204.19	469-61-4	0.02	
36	16.75	δ -Cadinene	204.19	483-76-1	11.04	
37	16.89	α -Curcumene	202.17	644-30-4	0.29	
38	17.15	α -Cadinene	204.19	24406-05-1	0.39	
39	17.58	cis-Calamenene	202.17	483-77-2	2.02	
40	21.04	6-Isopropyl-1,4- dimethylnaphthalene	198.14	489-77-0	0.03	

Table 1. Cont.

NO.	TR/min	Compound	MW	CAS	Content/%	Structure
41	21.49	Dimethyl phthalate	194.06	131-11-3	0.32	
42	22.14	Cadalene	198.14	483-78-3	0.01	
43	25	n-Hexadecanoic acid	256.24	57-10-3	0.13	
44	25.74	Erucamide	337.33	112-84-5	0.23	

γ -Terpinene (0.66%) is also a terpene, and although its relative content in *P. zhennan* leaves is low, it has strong antioxidant activity and xanthine oxidase inhibitory capacity with borneol acetate [38]. γ -Terpinene has antioxidant potential, with an IC_{50} against DPPH of only $122 \pm 2.5 \mu\text{g/mL}$ [39]. Both α -curcumene (0.29%) and β -bourene (0.09%) belong to sesquiterpenes. Although they account for only 0.35% and 0.32% of anhydrous ethanol extract, α -curcumene has a certain inhibitory effect on *Escherichia coli* and *Staphylococcus aureus* [40]. β -Bourenes shows a wide range of antibacterial activity against Gram-positive and Gram-negative bacteria and three pathogenic fungi [41].

The antioxidant activity of *P. zhennan* leaves may result from the combined effects of its compounds. Considering the year-round harvest ability and short-term reproducibility of *P. zhennan* leaves, they have potential medicinal value. However, this study did not fractionally extract the active components of *P. zhennan* leaves, and its antioxidant mechanism has not been fully revealed. In the future, we can consider further research in this direction.

4. Conclusions

It was determined that the *P. zhennan* leaves have strong antioxidant activity through in vitro antioxidant activity methods. Furthermore, based on HS-SPME-GC-MS analysis, 44 compounds, mainly terpenoids, were identified from *P. zhennan* leaves in this paper. *P. zhennan* leaves have potential medicinal value. Other properties, such as toxicology, should be evaluated before they can be used in humans. In addition, this study had some limitations. Fractional extraction of the active components of *P. zhennan* leaves was not performed. Thus, the antioxidant mechanism has not been fully revealed, and an in-depth study in this direction can be considered in the future.

Author Contributions: Conceptualization, methodology, L.Y. and W.C.; validation, L.Y., W.C., M.T. and X.C.; formal analysis, L.Y., W.C., M.Y. and X.M.; resources, M.T., X.C., M.Y. and X.M.; writing—original draft preparation, L.Y. and W.C.; writing—review and editing, W.C., M.T. and X.C.; investigation, visualization, supervision, Z.W. and X.W. All authors have read and agreed to the published version of the manuscript.

Funding: This work was supported by the National Natural Science Foundation of China (31870613 and 32160413), the High-level Innovative Talents Training Plan Project of Guizhou Province of China ([2016]5661), and the Outstanding Youth Science and Technology Talent Project of Guizhou Province of China (YQK[2023]003), International Joint Research Center for Biomass Materials Open Fund (2023-GH05) and Supported by the 111 Project (D21027).

Data Availability Statement: The data presented in this study are available upon reasonable request from the corresponding author.

Conflicts of Interest: The authors declare no conflicts of interest.

References

1. Yuan, X.; Wang, L.; Hu, M.; Zhang, L.; Chen, H.; Zhang, D.; Wang, Z.; Li, T.; Zhong, M.; Xu, L.; et al. Oxygen Vacancy-Driven Reversible Free Radical Catalysis for Environment-Adaptive Cancer Chemodynamic Therapy. *Angew. Chem. Int. Ed.* **2021**, *60*, 20943–20951. [[CrossRef](#)]
2. Jin, K. Modern biological theories of aging. *Aging Dis.* **2010**, *1*, 72–74.
3. Chen, X.; Yu, H.; Li, Z.; Ye, W.; Liu, Z.; Gao, J.; Wang, Y.; Li, X.; Zhang, L.; Alenina, N.; et al. Oxidative RNA damage in the pathogenesis and treatment of type 2 diabetes. *Front. Physiol.* **2022**, *13*, 725919. [[CrossRef](#)] [[PubMed](#)]
4. Lee, Y.T.; Chen, Y.L.; Wu, Y.H.; Chen, I.S.; Chang, H.S.; Wang, Y.H.; Chang, S.H.; Wu, Y.H.; Kao, T.I.; Yu, H.P.; et al. Meso-Dihydroguaiaretic Acid Ameliorates Acute Respiratory Distress Syndrome through Inhibiting Neutrophilic Inflammation and Scavenging Free Radical. *Antioxidants* **2022**, *11*, 123. [[CrossRef](#)] [[PubMed](#)]
5. Srivastava, K.K.; Kumar, R. Stress, oxidative injury and disease. *Indian J. Clin. Biochem.* **2015**, *30*, 3–10. [[CrossRef](#)] [[PubMed](#)]
6. Akhtar, M.; Rafiullah, M.; Shehata, W.; Hossain, A.; Ali, M. Comparative phytochemical, thin layer chromatographic profiling and antioxidant activity of extracts from some Indian herbald rugs. *J. Bioresour. Bioprod.* **2022**, *7*, 128–134. [[CrossRef](#)]
7. Hu, Y.; Zhang, L.; Feng, Y.; Pan, H. Preparation of tannic acid modified cellulose colorimetric test paper for Fe³⁺ and Ag⁺ detection. *J. For. Eng.* **2023**, *8*, 108–114.
8. El-Sherbiny, G.M.; Gazelly, A.; Sharaf, M.H.; Moghannemm, S.A.; Shehata, M.E.; Ismail, M.; El-Hawary, A.S. Exploitation of the antibacterial, antibiofilm and antioxidant activities of *Salvadora Persica* (Miswak) extract. *J. Bioresour. Bioprod.* **2023**, *8*, 59–65. [[CrossRef](#)]
9. Aung, T.; Bibat, M.A.D.; Zhao, C.C.; Eun, J.B. Bioactive compounds and antioxidant activities of *Quercus salicina* Blume extract. *Food Sci. Biotechnol.* **2020**, *29*, 449–458. [[CrossRef](#)]
10. Chia, T.Y.; Gan, C.Y.; Murugaiyah, V.; Hashmi, S.F.; Fatima, T.; Ibrahim, L.; Abdulla, M.H.; Alswailmi, F.K.; Johns, E.J.; Ahmad, A. A Narrative Review on the Phytochemistry, Pharmacology and Therapeutic Potentials of *Clinacanthus nutans* (Burm.f.) Lindau Leaves as an Alternative Source of Future Medicine. *Molecules* **2021**, *27*, 139. [[CrossRef](#)]
11. Abang, S.; Wong, F.; Sarbatly, R.; Sariau, J.; Baini, R.; Besar, N. Bioplastic classifications and innovations in antibacterial, antifungal, and antioxidant applications. *J. Bioresour. Bioprod.* **2023**, *8*, 361–387. [[CrossRef](#)]
12. Shan, S.; Ji, W.; Huang, Y.; Yu, Y.; Zhang, S.; Yu, W. Surface color regulation of white oak veneers based on polyphenol-iron complexation. *J. For. Eng.* **2023**, *8*, 182–189.
13. Bicas, J.L.; Neri-Numa, I.A.; Ruiz, A.; Carvalho, J.E.D.; Pastore, G.M. Evaluation of the antioxidant and antiproliferative potential of bioflavors. *Food Chem. Toxicol.* **2011**, *49*, 1610–1615. [[CrossRef](#)] [[PubMed](#)]
14. Chen, W.C.; Wang, S.W.; Li, C.W.; Lin, H.R.; Yang, C.S.; Chu, Y.C.; Lee, T.H.; Chen, J.J. Comparison of various solvent extracts and major bioactive components from *Portulaca oleracea* for antioxidant, Anti-Tyrosinase, and Anti- α -Glucosidase Activities. *Antioxidants* **2022**, *11*, 398. [[CrossRef](#)] [[PubMed](#)]
15. Li, X. 2-Phenyl-4,4,5,5-tetramethylimidazoline-1-oxyl3-oxide (PTIO \bullet) radical scavenging: A new and simple antioxidant assay in vitro. *J. Agric. Food Chem.* **2017**, *65*, 6288–6297. [[CrossRef](#)] [[PubMed](#)]
16. Pulido, R.; Bravo, L.; Saura, C.F. Antioxidant activity of dietary polyphenols as determined by a modified ferricreducing/antioxidant power assay. *J. Agric. Food Chem.* **2000**, *48*, 3396–3402. [[CrossRef](#)] [[PubMed](#)]
17. Ghorbel, A.; Fakhfakh, J.; Brieades, V.; Halabalaki, M.; Fontanay, S.; Duval, R.E.; Mliki, K.; Sayadi, S.; Allouche, N. Chemical Composition, Antibacterial Activity using Micro-broth Dilution Method and Antioxidant Activity of Essential Oil and Water Extract from Aerial Part of Tunisian *Thymus algeriensis* Boiss. & Reut. *J. Essent. Oil Bear. Plants* **2021**, *24*, 1349–1364.
18. Chai, T.T.; Kwek, M.T.; Ong, H.C.; Wong, F.C. Water fraction of edible medicinal fern *Stenochlaena palustris* is a potent α -glucosidase inhibitor with concurrent antioxidant activity. *Food Chem.* **2015**, *186*, 26–31. [[CrossRef](#)]
19. Huang, S.; Zhong, W.; Zhang, X.; Li, S.; Cai, X. Research progress of photochemical-based aggregation-induced luminescent materials. *J. For. Eng.* **2022**, *7*, 34–45.
20. Kostka, T.; Ostberg-Potthoff, J.J.; Stärke, J.; Guigas, C.; Matsugo, S.; Stojanov, L.; Velickovska, S.K.; Winterhalter, P.; Esatbeyoglu, T.; Mireeski, V. Bioactive phenolic compounds from Lingonberry (*Vaccinium vitis-idaea* L.): Extraction, chemical characterization, fractionation and cellular antioxidant activity. *Antioxidants* **2022**, *11*, 467. [[CrossRef](#)]
21. Wang, Y.; Wu, J.; Shen, R.; Li, Y.; Ma, G.; Qi, S.; Wu, W.; Jin, Y.; Jiang, B. A mild iodocyclohexane demethylation for highly enhancing antioxidant activity of lignin. *J. Bioresour. Bioprod.* **2023**, *8*, 306–317. [[CrossRef](#)]
22. Peng, J.; Yan, C.; Yang, F.; Hong, M.; Yang, Z.; Du, G.; Zhou, X. Preparation of tannin-urea-formaldehyde resin by carbonated tannin and its bonding properties. *J. For. Eng.* **2023**, *8*, 119–125.
23. Ayres, G.H. Evaluation of accuracy in photometric analysis. *J. Anal. Chem.* **1949**, *21*, 652–657. [[CrossRef](#)]
24. Tilahun, B.; Sosina, G.; Ajay, V.C.; Tarekegn, B.; Anurag, S.; Ashutosh, U. Comparative Study on Chemical Composition and Antioxidant Properties (GraphPad Prism Approach) of Wild Ethiopian *Z. spina-christi* and Indian *Z. jujube* Fruit Species. *J. Food Anal. Methods* **2022**, *15*, 2224–2237.
25. Wojtunik-Kulesza, A. Approach to Optimization of FRAP Methodology for Studies Based on Selected Monoterpenes. *Molecules* **2020**, *25*, 5267. [[CrossRef](#)] [[PubMed](#)]
26. Rahimmalek, M.; Szumny, A.; Gharibi, S.; Pachura, N.; Miroliaei, M.; Łyczko, J. Chemical Investigations in *Kelussiaod oratissima* Mozaff. Leaves Based on Comprehensive Analytical Methods: LC-MS, SPME, and GC-MS Analyses. *Molecules* **2023**, *28*, 6140. [[CrossRef](#)] [[PubMed](#)]

27. Li, Y.; Tan, B.; Cen, Z.; Fu, Y.; Wu, H. The variation in essential oils composition, phenolic acids and flavonoids is correlated with changes in antioxidant activity during *Cinnamomum loureirii* bark growth. *J. Arab. J. Chem.* **2021**, *14*, 103249. [[CrossRef](#)]
28. Ban, M.M.; Fan, Z.Y.; Zhang, D.Y.; Yang, L.; Zheng, Y.D.; Yang, B.B. Study on The Identification of *Amomum Villosum* Varieties. *Tradit. Chin. Drug Res. Clin. Pharmacol.* **2022**, *33*, 1407–1414.
29. Xu, H.N.; Mu, Y.; Zhang, Z.H.; Zhang, Z.; Zhang, D.Y.; Tan, X.Q.; Shi, X.B.; Liu, Y. Extraction and Identification of Volatiles from *Artemisia Argyi* and *Torilisscabra* and Their Effects on The Selectivity of Med Cryptic Adults of *Bemisia Tabaci* (Gennadius). *Acta Entomol. Sin.* **2022**, *65*, 343–350.
30. Carneiro, N.S.; Alves, C.C.F.; Alves, J.M.; Egea, M.B.; Martins, C.H.G.; Silva, T.S.; Bretanha, L.C.; Balleste, M.P.; Micke, G.A.; Silveira, E.V.; et al. Chemical composition, antioxidant and antibacterial activities of essential oils from leaves and flowers of *Eugenia klotzschiana* Berg (Myrtaceae). *An. Acad. Bras. Cienc.* **2017**, *89*, 1907–1915. [[CrossRef](#)]
31. Yang, J.B.; Tang, X.Y.; Cheng, W.Q. Research Progress on Biological Activity of α -Copaene and Its Derivatives. *J. China Prescr. Drug* **2015**, *13*, 12–13.
32. Ynag, M.D.; Xu, Q.X.; Ye, L.B.; Li, M.; Feng, Y.; Cheng, W.Q. Studies on The Synthesis of α -Copaene Derivatives, Screening of Anti-Tumor Cell Activity and Computer-Aided Drug Design. *China J. Chin. Mater. Medica* **2018**, *43*, 1001–1007.
33. Hu, J.H.; Han, J.; Li, Q.R.; Liu, T. Synthesis and comprehensive utilization of α -Copaene derivatives. *Shandong Chem. Ind.* **2014**, *43*, 64–68.
34. Medini, H.; Elaissi, A.; Khouj, M.L.; Alessandra, P.; Silvia, P.; Danilo, F.; Bruno, M.; Farhat, F.; Rachid, C. Chemical composition of the essential oils of the berries of *Juniperus oxycedrus* L. ssp. *Rufescens* (LK) and *Juniperus oxycedrus* L. ssp. *Macrocarpa* (S.&M.) Ball. And their antioxidant activities. *J. Nat. Prod. Res.* **2012**, *26*, 810–820.
35. Hussain, A.I.; Anwar, F.; Chatha, S.A.S.; Jabbar, A.; Mahboob, S.; Nigam, P.S. Rosmarinus officinalis essential oil: Antiproliferative, antioxidant and antibacterial activities. *J. Braz. J. Microbiol.* **2010**, *41*, 1070–1078. [[CrossRef](#)] [[PubMed](#)]
36. Dahham, S.S.; Tabana, Y.M.; Iqbal, M.A.; Ahamed, M.B.K.; Ezzat, M.O.; Majid, A.S.A.; Majid, A.M.S.A. The anticancer, antioxidant and antimicrobial properties of the sesquiterpene β -caryophyllene from the essential oil of *Aquilaria crassna*. *J. Mol.* **2015**, *20*, 11808–11829. [[CrossRef](#)] [[PubMed](#)]
37. Tele, A.M.; Silva-Silva, J.V.; Fernande, J.M.P.; Calabrese, K.D.S.; Abreu-Silva, A.L.; Marinho, S.C.; Mouchrek, A.N.; Filho, V.E.M.; Almeida-Souza, F. *Aniba rosaeodora* (Var. *amazonica* Ducke) essential oil: Chemical composition, antibacterial, antioxidant and antitrypanosomal activity. *J. Antibiot.* **2020**, *10*, 24. [[CrossRef](#)]
38. Liu, X.; Gao, B.; Dong, Z.; Qiao, Z.; Yan, M.; Han, W.; Li, W.; Han, L. Chemical Compounds, Antioxidant Activities, and Inhibitory Activities against Xanthine Oxidase of the Essential Oils from the Three Varieties of Sunflower (*Helianthus annuus* L.) Receptacles. *Front. Nutr.* **2021**, *8*, 3389. [[CrossRef](#)]
39. Tepe, B.; Sihoglu-Tepe, A.; Daferera, D. Chemical composition and antioxidant activity of the essential oil of *Clinopodium vulgare* L. *J. Food Chem.* **2007**, *103*, 766–770. [[CrossRef](#)]
40. Wang, X.; Shen, Y.; Thakur, K.; Han, J.; Zhang, J.G.; Hu, F.; Wei, Z.J. Antibacterial Activity and Mechanism of Ginger Essential Oil against *Escherichia coli* and *Staphylococcus aureus*. *Molecules* **2020**, *25*, 3955. [[CrossRef](#)]
41. Liu, X.L. Identification of volatile components in *Phyllanthus emblica* L. and their antimicrobial activity. *J. Med. Food* **2009**, *12*, 423–428. [[CrossRef](#)] [[PubMed](#)]

Disclaimer/Publisher’s Note: The statements, opinions and data contained in all publications are solely those of the individual author(s) and contributor(s) and not of MDPI and/or the editor(s). MDPI and/or the editor(s) disclaim responsibility for any injury to people or property resulting from any ideas, methods, instructions or products referred to in the content.